ISSN 0021-3640, JETP Letters, 2015, Vol. 101, No. 5, pp. 308–312. © Pleiades Publishing, Inc., 2015.
Original Russian Text © A.A. Ionin, S.I. Kudryashov, S.V. Makarov, P.N. Saltuganov, L.V. Seleznev, D.V. Sinitsyn, V.A. Lednev, S.M. Pershin, 2015, published in Pis'ma v Zhurnal Eksperimental'noi i Teoreticheskoi Fiziki, 2015, Vol. 101, No. 5, pp. 336–341.

Electron Emission and Ultrafast Low-Fluence Plasma Formation during Single-Shot Femtosecond Laser Surface Ablation of Various Materials¶

A. A. Ionin[a], S. I. Kudryashov[a, b, *], S. V. Makarov[a, e], P. N. Saltuganov[a, c], L. V. Seleznev[a], D. V. Sinitsyn[a], V. A. Lednev[d], and S. M. Pershin[d]

[a] *Lebedev Physical Institute, Russian Academy of Sciences, Moscow, 119991 Russia*
* *e-mail: sikudr@lebedev.ru*
[b] *National Research Nuclear University MEPhI, Moscow, 115409 Russia*
[c] *Moscow Institute of Physics and Technology (State University) MIPT, Dolgoprudnyi, Moscow region, 141700 Russia*
[d] *Prokhorov General Physics Institute, Russian Academy of Sciences, Moscow, 119991 Russia*
[e] *ITMO University, St. Petersburg, 197101 Russia*

Received October 22, 2014; in final form, January 21, 2015

Emission of erosive plasma has been observed during electric probe and optical emission spectral measurements of plumes produced by single-shot femtosecond laser ablation of optical-quality surfaces of various materials—copper, titanium, and silicon—at laser fluences well below the corresponding thermal ablation thresholds, replacing presumably electron emission at lower fluences. The onset of erosive plasma correlates on the fluence scale with saturation of dependences of self-reflectivity of the pumping femtosecond laser pulses, reflecting the "freezing" of electron dynamics (variation of electron density or temperature) during the pumping pulses, despite the monotonically increasing laser fluences.

DOI: 10.1134/S0021364015050112

1. Traditionally, low-fluence thermal ablation of material surfaces by short (pico-, nano-, and microsecond) laser pulses is considered as preceding their high-fluence erosive plasma formation [1–3]; such plasma onset is usually initiated by optical breakdown within an ablative thermal plume [3]. This viewpoint is also typical for ablation by ultrashort (mostly, femtosecond) laser pulses [4, 5], even though in this case thermal dynamics is preceded by high-temperature electronic dynamics and electron emission [6–8], with the latter saturating at low fluences $F \sim 1$–10 mJ/cm^2 because of the blocking effect of the related electron space charge [6]. As a result, electron emission is considered to be saturated over the broad femtosecond laser fluence range from low (~mJ/cm^2) to moderately high (~J/cm^2) fluences, approaching the electron-ion plasma formation regime ($F \gg 10$ J/cm^2) [9], and for this reason was typically neglected in the energy balance of ultrafast electronic dynamics [10].

Meanwhile, during the last years, a nonlinear yield of charged particles (electrons, positive and negative ions) was observed for diverse materials even for moderate (~0.1 J/cm^2) fluences of single and multiple femtosecond laser pulses [7, 11–16]. Although this effect was not explicitly explained, even being related to multishot surface nanostructuring below the corresponding thermal ablation threshold [13, 14], apparently, expansion of such a quasi-neutral electron-ion double electric layer can avoid the blocking effect of the electron space charge, yielding formation of thin surface erosive plasma even at low $F \sim 0.1$–1 J/cm^2. Hence, there appear new experimental opportunities for ultrafast nano-deep femtosecond laser ablation and nanoscale surface structuring owing to the reduced energy transport on the surface, while such surface plasma will degrade the mass density contrast of surfaces during their interaction with femtosecond laser pulses of sub- and relativistic intensity.

In this letter, we report on a systematic study of charged particle emission from copper, titanium, and silicon surfaces during their single-shot femtosecond laser ablation using an original low-vacuum collecting electrical scheme and optical emission spectroscopy of ablative plumes, accompanied by self-reflection measurements for pumping femtosecond laser pulses to track ultrafast electronic dynamics during the photoexcitation.

2. In these studies, single-shot ablation of different samples—an unprotected 25-nm-thick copper mirror, an optical-quality titanium foil mechanically polished using a polishing powder with the grain size of ≈150 nm, and an atomically smooth undoped Si(100) wafer 0.45 mm thick with a natural oxide layer 2–3 nm

¶The article was translated by the authors.

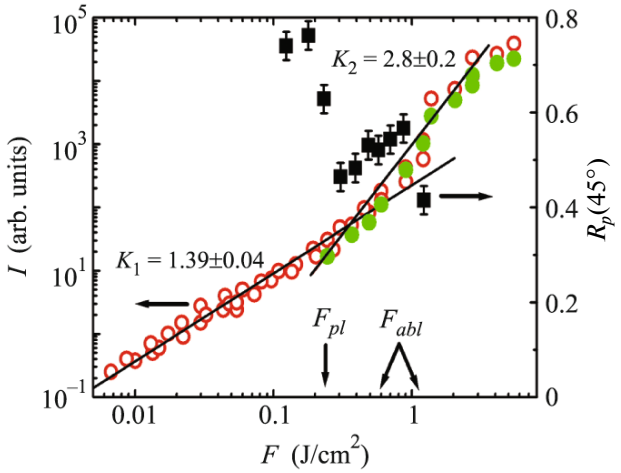

Fig. 1. (Color online) (Left axis) Experimental fluence dependences of (open red circles) electron and (green circles) ion emission signals $I(F)$ for copper in double logarithmic coordinates with the linear approximation of the former data with slopes $K_{1,2}$. (Right axis) Experimental fluence dependence of the self-reflection coefficient $R_P(45°)$ for copper (dark squares). The vertical arrows denote the experimentally measured plasma formation threshold F_{pl} and the known single-shot thermal ablation thresholds $F_{abl} \approx 0.6$ and 1.1 ± 0.1 J/cm^2 [17, 18].

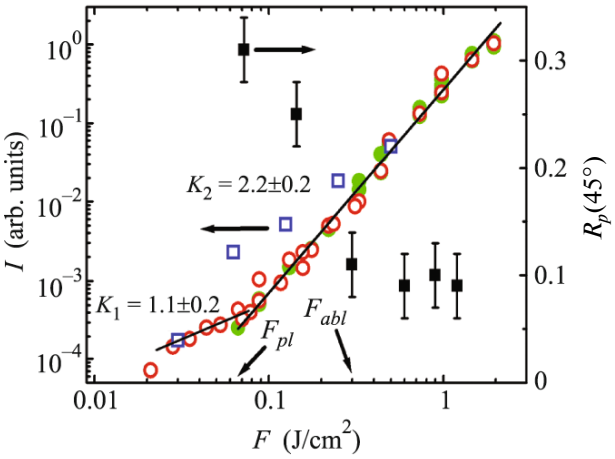

Fig. 2. (Color online) (Left axis) Experimental fluence dependences of (open red circles) electron and (green circles and open blue circles, TiII 336 nm) ion emission signals $I(F)$ for titanium in double logarithmic coordinates with the linear approximation of the former data with slopes $K_{1,2}$. (Right axis) Experimental fluence dependence of the self-reflection coefficient $R_P(45°)$ for titanium (dark squares). The vertical arrows denote the experimentally measured plasma formation threshold F_{pl} and the known single-shot thermal ablation thresholds $F_{abl} \approx 0.28$ and 0.3 J/cm^2 [17, 19].

thick—was performed by means of an electromechanical shutter and pulse-to-pulse translation of the samples arranged on a three-dimensional PC-controlled motorized translation stage. Prior to laser irradiation, the sample surface was cleaned by treatment in an ultrasonic bath (DR-LQ13) in a surfactant solution (WeberMS) for 5 min, while plasma cleaning (SC7620, Quorum) was not done prior to such low-vacuum studies. Laser irradiation was provided by single pulses of a Ti:sapphire laser (wavelength 744 nm, FWHM $\tau_{las} \approx 100$ fs, pulse energy in the TEM_{00}-mode up to 8 mJ, repetition rate 10 Hz) focused by an uncoated spherical silica lens (BK-7, $f = 50$ mm) into an elliptical spot with its characteristic $1/e$ radii $\approx$0.10 mm and $\approx$0.05 mm [7, 11, 12]. The pulse energy was smoothly diminished by means of a half-wave plate and Glan prism polarizer, starting from $\approx$0.3 mJ, to avoid laser beam degradation via self-focusing in air (the critical self-focusing power in air at 744 nm was $\approx$3 GW, corresponding to $\approx$ 0.3 mJ for the 100-fs laser pulses) and scattering/refraction in air breakdown plasma.

Self-reflection of pumping femtosecond laser pulses was measured in ambient air using the optical scheme reported elsewhere [7, 8]. Then, two calibrated pyroelectric calorimeters were used to acquire energies of the obliquely incident (the incidence angles—20° or 45°) p-polarized and reflected femtosecond laser pulses.

In the collecting electrical scheme [7, 8, 11, 12], a stationary copper collecting electrode with a 4-mm hole and electrical potential of $\pm$(0–300) V was arranged inside an evacuated gas cell at the distance of 1 mm from the sample, arranged on the grounded electrode, while the entire set was arranged on the three-dimensional PC-controlled motorized translation stage. Femtosecond laser pulses were focused through an optical window of the cell and the inner hole of the collecting electrode by a silica lens at their normal incidence. In ambient air, the emitted electrons were trapped by oxygen molecules on a nanosecond timescale and then slowly drifted as negative ions in the applied electric field toward the collector on a sub-millisecond timescale, inducing there an image current (potential) I, acquired using a megaohm input of a storage oscilloscope [7, 11, 12]. Alternatively, fast nanosecond (FWHM duration $\approx$5 ns) image currents were detected using its 50-ohm input [8].

Additionally, spectral measurements of spatiotemporal emission dynamics were performed for ablative plumes in the femtosecond laser fluence range $F =$ 0.015–1.5 J/cm^2 in back-reflection geometry, using two fused-silica lenses for frontal imaging of plumes to an entrance slit of a Spectro-Physics 74050 spectrometer equipped with an Andor iStar ICCD camera. As a result, optical spectra of ablative plumes were acquired at a temporal resolution as high as 3 ns over the spectral range of 200–600 nm, where the most intense atomic and ionic spectral lines are situated.

3. The acquired dependences of image currents I on F for all materials used appear similar (Figs. 1–3). For low $F < F_{pl}$, where their thresholds F_{pl} vary from

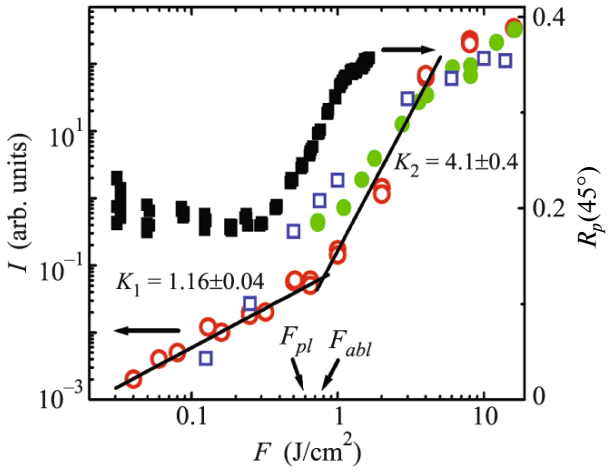

Fig. 3. (Color online) (Left axis) Experimental fluence dependences of (open red circles) electron, (green circles) ion, and (open blue circles, SiI 288 nm) atomic emission signals $I(F)$ for silicon in double logarithmic coordinates with the linear approximation of the first data with slopes $K_{1,2}$. (Right axis) Experimental fluence dependence of the self-reflection coefficient $R_P(45°)$ for silicon (dark squares). The vertical arrows denote the experimentally measured plasma formation threshold F_{pl} and the known single-shot thermal ablation threshold $F_{abl} \approx 0.75$ J/cm^2 [20].

0.2 to 0.6 J/cm^2, these currents exhibit electron character (thermionic, photo-, or combined emission mechanisms), verified through complete suppression of such emission by changing polarity of the collector potential to negative, and almost linear yield $I_e \propto F$. Then, upon exceeding F_{pl}, a nonlinear intense—by three to four orders of magnitude—increase in charge emission occurred in the form $I_{ei} \propto F^{\gamma}$, where the exponent γ varies in the range of 2–4 (Figs. 1–3). The character and amplitude of charged particle emission were almost independent of the potential polarity for the collecting electrode, indicating the presence of both—electron and ion—components of the image currents I_{ei}. Surprisingly, single-shot thermal ablation thresholds F_{abl} for these materials exceed their magnitudes F_{pl}: for copper, $F_{abl} \approx 0.6$ J/cm^2 [15, 17, 18] versus $F_{pl} \approx 0.25$ J/cm^2 (Fig. 1); for titanium, $F_{abl} \approx 0.3$ J/cm^2 [17, 19] versus $F_{pl} \approx 0.07$ J/cm^2 (Fig. 2); for silicon, $F_{abl} \approx 0.75$ J/cm^2 [20] versus $F_{pl} \approx 0.6$ J/cm^2 (Fig. 3). In all these cases, we considered the high-temperature ablation in the form of hydrodynamic plasma-vapor-droplet expansion of supercritical fluid, rather than subcritical spallation ablation in the form of nanometer-thick microscale fragments of the spalled molten layer [20].

To reveal the dynamics of such charge emission, we considered the correlation between the fluence dependences of emission signals and of pump-pulse self-reflectivity (R_P) (Figs. 1–3). In contrast with expected monotonic changes, the latter dependences demonstrate saturation of decreasing self-reflectivity for the metals (Figs. 1, 2) and increasing self-reflectivity for silicon (Fig. 3), starting from F_{pl}. Such reflectivity saturation in this fluence range was often observed for different metals [21–24]; however, without charge emission measurements, it was not related to some specific physical effects. For examples, for semiconductors, such plateau of increased reflectivity was earlier frequently observed and studied for almost three decades, being assigned to ultrafast nonthermal structural disordering of semiconductors and semimetals [25–28] or ultimate electronic renormalization of their band spectrum [7]. Direct comparison of plasma emission and reflectivity changes indicates that such stabilization, even "freezing" of electronic dynamics for $F > F_{pl}$, is unambiguously related to formation of the plasma and can be considered as a first-order electronic evaporative transition. Such transition stabilizes parameters of the electronic system via removal of excessive energy through plasma emission in the specific fluence range. At higher fluences $F \sim 1$–10 J/cm^2, the electron density and thickness of such surface plasma can approach values sufficient for surface screening, with presumable laser absorption and heating in the surface plasma rather than in the material, as is known from optical reflectivity measurements over the entire fluence range of 0.1–10^3 J/cm^2 [21–24]. It is noteworthy that such a plasma-mediated ablation mechanism was proposed in theory earlier, but it appearance was related to much higher fluences $F \sim 10$ J/cm^2 [5]. Similarly, such anomalies in energy spectra of electrons and ions—e.g., the presence of high-energy (~1 keV) and low-energy (~1 eV) components—were experimentally observed in mass spectra of quasi-neutral femtosecond laser ablation products for copper and gold, with a similar slope (≈3) and similar threshold (≈0.3–0.4 J/cm^2) of ion yield for copper [15] (cf. Fig. 1).

Since the deposited energy density on the surface for $F \approx F_{pl}$ is lower than ~10 eV/atom, the plasma-mediated surface ablation is negligible in the surface relief in comparison with the laser penetration depth (~10 nm) [8]. On the contrary, the much more sensitive optical emission spectroscopy of ablative plumes indicates a drastic rise of the singly charged titanium ion yield at zero acquisition delay [29] (Fig. 4), starting from F_{pl} (Figs. 2, 3). The plasma origin of the titanium ion lines [29] in Fig. 4 is strongly supported by the intense plasma emission continuum with its temperature of ~1 eV, while the appearance of atomic lines in the region >400 nm is related to plasma radiative recombination.

As mentioned above, the observed effect opens new possibilities for ultrafast, nanoscale femtosecond laser ablation of material surfaces for their ultraprecise processing or nanosampling in microanalysis. On the other hand, during such prompt plasma-mediated

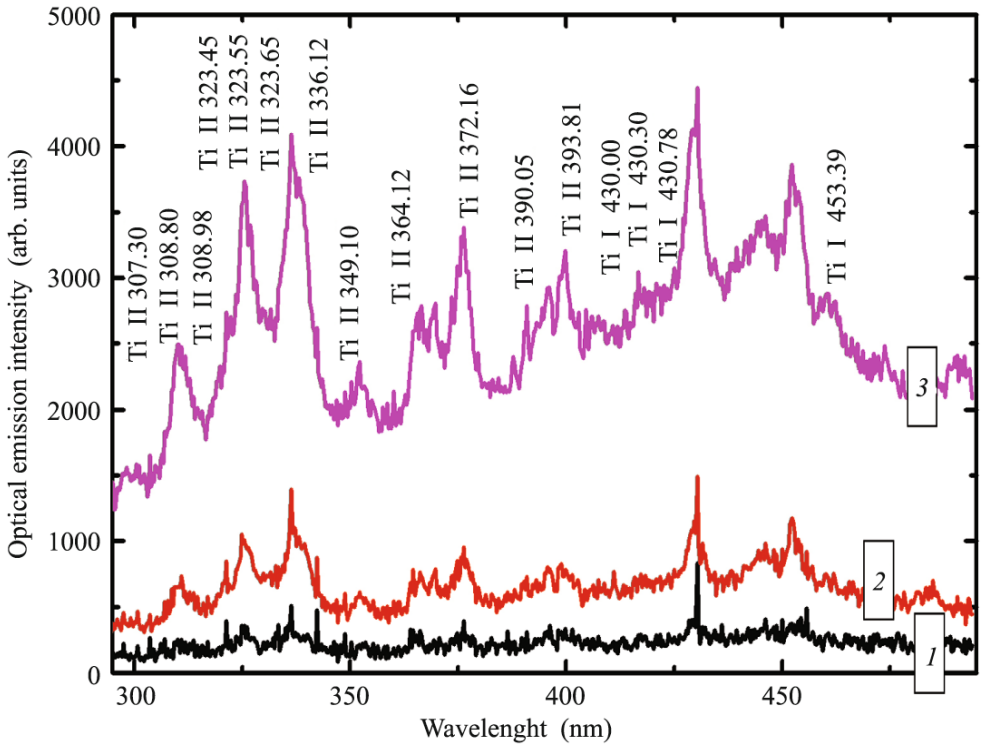

Fig. 4. (Color online) Spectra of ablative plume for titanium at $F \approx$ (*1*) 0.06, (*2*) 0.125, and (*3*) 0.25 J/cm^2 at zero delay of the acquisition pulse of 10-ns duration. The spectral line assignment was performed following [29].

femtosecond laser ablation, the effects of energy transport inside the sample become strongly reduced in favor of stronger energy localization in the absorbing layer. This enables material removal exactly from the corresponding focal spot, accounting for some more significant localization of the ablation due to its threshold-like character ($F > F_{pl}$).

Moreover, the observed plasma-mediated femtosecond laser ablation regime is filling the gap between the corresponding regimes of thermionic/photoemission of electrons at low fluences and low-temperature ablative plasma formation at high fluences. Importantly, both of these extreme states of matter—a solid conductor with its electron temperature well below the corresponding Fermi one (T_F) and plasma with its temperature of several T_F—are rather well characterized systems, while the intermediate state is usually described only by extrapolating dependences known for one of the extreme states or by interpolation between those states. Therefore, enlightening the phenomenological picture of the intermediate matter state, generated by femtosecond laser excitation, is very important to develop a universal theoretical model of all these states.

Finally, the observed effect of low-fluence femtosecond laser formation of surface plasma may result in preplasma formation by low-intensity femtosecond laser prepulses during interaction of femtosecond laser pulses with sub- and relativistic intensities with solid targets, deteriorating their mass-density contrast.

4. Hence, the "freezing" effect was experimentally demonstrated for the first time in this work for high-temperature solid-state electronic dynamics driven by an intense femtosecond laser pulse because of low-threshold surface plasma formation with a nonlinear yield of charged particles during the heating ultrashort laser pulse. The aforementioned plasma formation and solid-state electron dynamics will be further studied by means of optical emission spectroscopy and time-resolved optical probing.

This work was partially supported by the Russian Foundation for Basic Research (project nos. 13-02-00971-a, 14-02-00460-a, and 14-02-00748), by the Presidium of the Russian Academy of Sciences (program no. 24), and by the Government of the Russian Federation (project no. 074-U01, ITMO Post-Doctoral Fellowship for S.V. Makarov).

REFERENCES

1. Yu. V. Afanas'ev, V. A. Isakov, and O. N. Krokhin, Sov. Phys. JETP **54**, 910 (1981).
2. J. M. Liu, R. Yen, H. Kurz, and N. Bloembergen, Appl. Phys. Lett. **39**, 755 (1981).
3. A. A. Ionin, S. I. Kudryashov, and L. V. Seleznev, Phys. Rev. E **82**, 016404 (2010).

4. S. I. Anisimov and B. S. Luk'yanchuk, Phys. Usp. **45**, 293 (2002).
5. E. G. Gamaly, A. V. Rode, B. Luther-Davies, and V. T. Tikhonchuk, Phys. Plasmas **9**, 949 (2002).
6. X. Y. Wang, D. M. Riffe, Y.-S. Lee, and M. C. Downer, Phys. Rev. B **50**, 8016 (1994).
7. A. A. Ionin, S. I. Kudryashov, S. V. Makarov, P. N. Saltuganov, L. V. Seleznev, D. V. Sinitsyn, and A. R. Sharipov, JETP Lett. **96**, 375 (2012).
8. A. A. Ionin, S. I. Kudryashov, S. V. Makarov, L. V. Seleznev, and D. V. Sinitsyn, Appl. Phys. A **117**, 1757 (2014).
9. S. I. Kudryashov, A. A. Ionin, S. V. Makarov, N. N. Mel'nik, L. V. Seleznev, and D. V. Sinitsyn, AIP Conf. Proc. **1464**, 244 (2012).
10. B. Y. Mueller and B. Rethfeld, Phys. Rev. B **87**, 035139 (2013).
11. M. A. Gubko, W. Husinsky, A. A. Ionin, S. I. Kudryashov, S. V. Makarov, C. Nathala, A. A. Rudenko, L. V. Seleznev, D. V. Sinitsyn, and I. V. Treshin, Laser Phys. Lett. **11**, 065301 (2014).
12. S. I. Kudryashov and N. N. Mel'nik, in *Graphite: Properties, Occurrences and Uses*, Ed. by Q. C. Campbell (Nova Science Publ., Washington, 2013), p. 69.
13. V. Schmidt, W. Husinsky, and G. Betz, Phys. Rev. Lett. **85**, 3516 (2000).
14. H. Dachraoui and W. Husinsky, Phys. Rev. Lett. **97**, 107601 (2006).
15. S. Amoruso, X. Wang, C. Altucci, C. de Lisio, M. Armenante, R. Bruzzese, N. Spinelli, and R. Velotta, Appl. Surf. Sci. **186**, 358 (2002).
16. M. Hada, D. Zhang, K Pichugin, J. Hirscht, M. A. Kochman, S. A. Hayes, S. Manz, R. Y. N. Gengler, D. A. Wann, T. Seki, G. Moriena, C. A. Morrison, J. Matsuo, G. Sciaini, and R. J. D. Miller, Nature Commun. **5**, 3863 (2014).
17. P. T. Mannion, J. Magee, E. Coyne, G. M. O'Connor, and T. J. Glynn, Appl. Surf. Sci. **233**, 275 (2004).
18. S. E. Kirkwood, A. C. van Popta, Y. Y. Tsui, and R. Fedosejevs, Appl. Phys. A **81**, 729 (2005).
19. Y. Me and C. P. Grigoropoulos, J. Appl. Phys. **89**, 5183 (2001).
20. A. A. Ionin, S. I. Kudryashov, L. V. Seleznev, D. V. Sinitsyn, A. F. Bunkin, V. N. Lednev, and S. M. Pershin, J. Exp. Theor. Phys. **116**, 347 (2013).
21. H. M. Milchberg, R. R. Freeman, S. C. Davey, and R. M. More, Phys. Rev. Lett. **61**, 2364 (1988).
22. M. K. Grimes, A. R. Rundquist, Y.-S. Lee, and M. C. Downer, Phys. Rev. Lett. **82**, 4010 (1999).
23. J. P. Colombier, P. Combis, E. Audouard, and R. Stoian, Phys. Rev. E **77**, 036409 (2008).
24. P. S. Komarov, S. I. Ashitkov, A. V. Ovchinnikov, D. S. Sitnikov, M. E. Veysman, P. R. Levashov, M. E. Povarnitsyn, M. B. Agranat, N. E. Andreev, and K. V. Khishchenko, J. Phys. A: Math. Theor. **42**, 214057 (2009).
25. C. V. Shank, R. Yen, and C. Hirlimann, Phys. Rev. Lett. **51**, 900 (1983).
26. H. W. Tom, G. D. Aumiller, and C. H. Brito-Cruz, Phys. Rev. Lett. **60**, 1438 (1988).
27. P. Saeta, J. K. Wang, Y. Siegal, N. Bloembergen, and E. Mazur, Phys. Rev. Lett. **67**, 1023 (1991).
28. K. Sokolowski-Tinten, J. Bialkowski, and D. von der Linde, Phys. Rev. B **51**, 14186 (1995).
29. http://physics.nist.gov/PhysRefData/ASD/lines_form.html